Hydration effect on interaction mode between glutamic acid and Ca^{2+} and its biochemical implication: a theoretical exploration†

Feng Xiang,[a] Ping Li,[a] Shihai Yan,[a] Lixiang Sun,[a] Robert I. Cukier[b] and Yuxiang Bu*[ab]

Received (in Montpellier, France) 4th January 2006, Accepted 23rd March 2006
First published as an Advance Article on the web 21st April 2006
DOI: 10.1039/b518408h

The stepwise hydration effect on the glutamic acid–Ca^{2+} (GC) complexes in the gas phase has been investigated by density functional theory (DFT) calculations. The thermodynamics parameters for the hydration reactions, the stepwise hydration energies and accurate geometries have been explored. To elucidate the Ca^{2+}–ligand interaction, the charge transfer, bonding analysis and IR spectroscopic characteristics have also been investigated. The correlating data have shown that all of the stepwise hydration reactions are enthalpy-driven because of the relatively small value of ΔS, but the number of coordinated water molecules in the first shell of Ca^{2+} is not limitless. In our study, the optimal coordination number (CN) of Ca^{2+} in the first shell is 6 or 7; the former value agrees well with the data reported in the Protein Data Bank (PDB), and the latter is the reflection of the most frequent Ca^{2+}-binding motif, EF-hand, in soluble proteins. Furthermore, the self-consistent reaction field (SCRF) and higher-level MP2 calculations have confirmed our conclusions. Additionally and very importantly, the stepwise hydration in either the first or second coordination shell can weaken the glutamic acid–Ca^{2+} interaction gradually till the glutamic acid ligand is replaced by the added water molecules, resulting in the conversion of coordination mode of the glutamic acid to Ca^{2+} from the inner-sphere one to a peripheral interaction mode, just like the ligand exchange process in the Ca^{2+} release channel existing in the real biological system. Finally, the similarities and discrepancies between our model and the Ca^{2+}-channel *in vivo* have been compared.

1. Introduction

Ca^{2+}-ATPase, which is also called Ca^{2+} pump and Ca^{2+}-channel, is a member of the P-type ATPases that transport calcium ions across membranes against a concentration gradient. As one of the important physiological phenomena, Ca^{2+}-ATPase can control muscle contraction and signal the metabolism of various cells *in vivo* efficiently.[1–4]

In past years, some related experimental and theoretical studies on Ca^{2+}-channel have been reported.[1–6] For example, Toyoshima *et al.* have solved the crystal structure of the Ca^{2+}-ATPase of skeletal muscle sarcoplasmic reticulum (SERCA1a) corresponding to the Ca^{2+}-bound state.[1] The possible function of every component and the mechanism of the Ca^{2+} ions transporting across the biological membranes have also been extensively studied by Lee's group.[2] Carloni and Costa have used molecular dynamics and electrostatic modelling to investigate the structural and dynamical features of key intermediates in the Ca^{2+} binding process of the protein.[5] The ion selectivity of the Ca^{2+}-ATPase has also been explored by Dudev *et al.*[6] Although significant progress has been made in exploring the activity of the Ca^{2+}-ATPase, the underlying molecular mechanisms are totally unclear, especially for the theoretical investigations associated closely with the interactive details of the Ca^{2+}-channel. In our previous study,[7] we investigated the interactive mechanism of how a Ca^{2+} ion interacts with a single glutamic acid residue (reported in the correlating paper,[2] the glutamic acid may be part of the Ca^{2+}-channel and can control its switch) in the gas phase. As a logical starting point, these studies can extend our understanding of how the calcium cations bind to the transmembrane α helices and how they transfer through Ca^{2+}-ATPase. The results reveal that there are 16 stable conformers of the glutamic acid–Ca^{2+} (GC) complexes and the preferred coordination mode in the gas phase is the tri- or bidentate form. However, it is well known that the organisms exist in the bulk solvent, and the solvent effects often play the important roles in determining the conformational preferences, energetic changes and other chemical or biochemical quantities. To date, the systematic studies about the GC complexes in solution have never been reported, despite its importance in biochemistry, to our best knowledge. As reported previously, one can learn directly about the influence of water on the metal–amino acid complexes from differences in the gas-phase and solution-phase structures.[8] In principle, the gap in our understanding between the gas-phase and solution-phase properties of biomolecules can be bridged by investigating

[a] *Institute of Theoretical Chemistry, Shandong University, Jinan 250100, P. R. China. E-mail: byx@sdu.edu.cn*
[b] *Department of Chemistry, Michigan State University, East Lansing, MI 48823, USA*

† Electronic supplementary information (ESI) available: B3LYP/6-31G(d,p) optimized complexes, high energy level orbitals, geometrical parameters and energy differences for the **1**- and **2**-series. See DOI: 10.1039/b518408h

how water changes the biomolecular structure, one water molecule at a time. Thus, in this paper, the stepwise hydration was used to simulate the hydration effects on the GC complexes to explore: (i) the conformational changes of the GC complexes upon hydration; (ii) the optimal coordination number (CN) for the studied system in the multi-ligand environment; (iii) the energetic effects with the increase in water molecules and (iv) the correlating biological applications.

Considering the facts that the bidentate coordination of the amino acid to Ca^{2+} is common in organisms,[9,10] the bidentate GC complexes, which are denoted as **1** and **2**, respectively (shown in Fig. 1), are selected from ref. 7 as the beginning point to study the further hydration effects. The same consideration has been taken in other papers.[6,18]

2. General considerations and computational details

2.1. General considerations

When detecting the hydration effects on the GC binding character, it is more practical to coordinate the water molecules to the most hydrophilic site directly, in spite of so many electronegative ones in the GC complexes. In order to find this

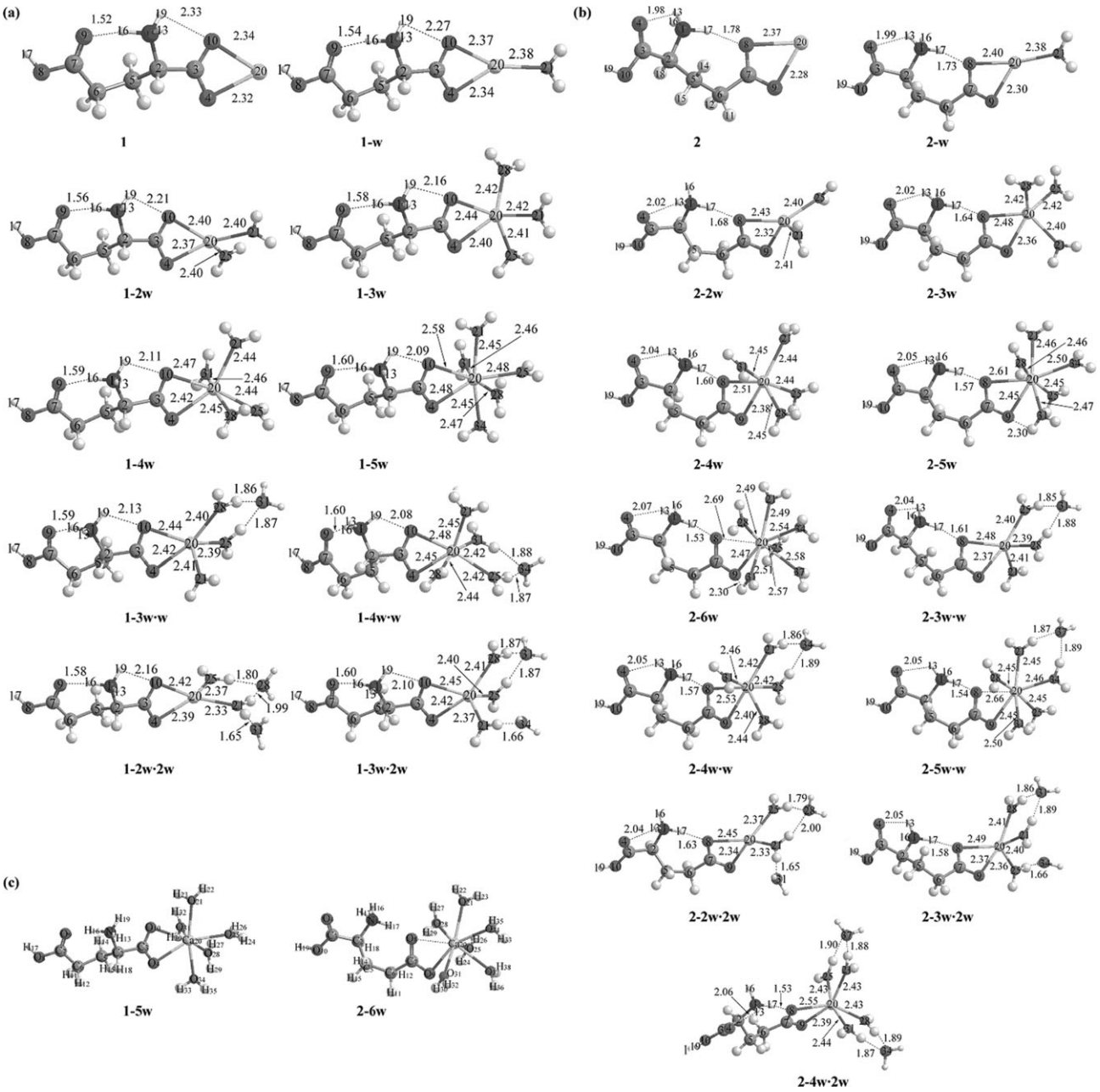

Fig. 1 B3LYP/6-31+G(d,p)-optimized multihydrated glutamic acid–Ca^{2+} complexes of the (a) **1**-series and (b) **2**-series corresponding to the global minima on the PES. Distances in the figure are given in angstroms. Here, only the labels for the heavy atoms and the main hydrogen atoms are presented. As representative complexes of the **1**- and **2**-series, **1-5w** and **2-6w** are selected to identify the atoms in section (c).

site, all of the possible monohydrated models of **1** and **2** have been calculated. The optimized geometries and relative energies are shown in Fig. S1 of the ESI.† Obviously, the Ca^{2+} ion end presents the strongest binding ability to water. Upon the monohydrated geometry, the second water molecule is coordinated to the Ca^{2+} site to establish the corresponding bihydrated complex. In this way, more coordinated water molecules are added stepwise to the calcium end to detect the details of the hydration processes.

Ca^{2+} exhibits a wide variation in the CN of the first-shell water molecules. A survey of calcium-binding sites composed of only amino acids and water molecules in the Protein Data Bank (PDB)[11] shows that the CN of Ca^{2+} in proteins varies from 6 to 9;[12] the average CN is six, while for an EF-hand site, which is the most frequent Ca^{2+}-binding motif in soluble proteins, it is seven.[13] In fact, site II of the high-affinity Ca^{2+}-binding sites of the Ca^{2+}-ATPase is reminiscent of EF-hand.[14] Considering these facts, the water molecules are added stepwise from 1 to 6 to the calcium end of the GC complexes, that is, the CN of Ca^{2+} varies from 3 to 8 correspondingly (including the two chelated carboxylic oxygen atoms).

With the increase of the steric repulsions, it can be speculated that the formation of the secondary solvent shell will take place when more water molecules are included. In the prevenient studies on the $Ca^{2+}\cdot(H_2O)_n$ system, Bernal-Uruchurtu and Ortega-Blake found that the corresponding CN for the second shell around Ca^{2+} was 20.[15] In this paper, only those geometries which have one or two water molecules in the secondary hydration shell were selected to investigate the peripheral hydration effects due to the limitation of the calculation method used here.

The idea designed in this paper is listed as follows: first, upon the investigatory results of ref. 7, we selected two GC complexes (**1** and **2**), both of which coordinate to Ca^{2+} in the bidentate form, as the initial geometries to carry out the further work. Second, the hydration of the first shell was investigated by stepwise addition of the water molecules, from 1 up to 6, to the Ca^{2+} end. Then, the water molecules were added to the second shell of Ca^{2+}, forming the first-and-second-shell coordination mode, to investigate the peripheral hydration. Finally, the SCRF method was employed to detect the geometrical and energetic changes of the complexes in the bulk solution.

In this work, two different nomenclatures are used to present the GCW complexes. One is the (n, m) form, in which there are n water molecules in the first coordination shell of Ca^{2+} and $m H_2O$ in the second one. In another nomenclatorial system, **1** and **2** refer to the unhydrated GC complexes derived from the ref. 7. As to ***a-nw***, the first number, ***a***, denotes the unhydrated GC complex, **1** or **2**; the second one, ***n***, is the number of coordinated water molecules. Finally, ***w*** is an abbreviation for water. For example, **1-3w** is the trihydrate derived from the initial isomer **1**.

2.2. Computational details

Two different levels of theory have been used:

(1) the Hartree–Fock (HF) method has been chosen for the initial geometry optimizations.

(2) Since the non-local three-parameter hybrid exchange B3LYP density functional method[16] is computationally less expensive and can provide many properties comparable in accuracy to experimental values, it has been applied successfully to the calculations of the similar hydration systems.[6,8,17–20] For example, Lim and co-workers have used the DFT/B3LYP method to investigate the processes of metal binding and selecting in metalloproteins, including the influence of the hydration effects.[6] Jockusch *et al*. have investigated the stepwise hydration of valine–alkali metal ion complexes, Val–$M^+\cdot(H_2O)_n$, n = 2–6, M = Li, Na, and K, at the B3LYP/6-311++G** level.[8] So in this paper, the B3LYP density functional method was used for both geometry and energy calculations of the GCW system. All geometry optimizations, at all wavefunction levels, were made without any symmetry constraints.

To further elucidate the geometry and energy characters of these complexes, three calculation steps were adopted. First, all hydrated forms were optimized at the HF/3-21G level. Then, these geometries were reoptimized at the B3LYP/6-31+G(d,p) level. Each stationary point was fully characterized as a genuine minimum at this theoretical level. Finally, the relevant energies and the other quantities were refined using the B3LYP/6-311++G(2d,p) singlet-point calculations at the B3LYP/6-31+G(d,p) geometries.

In this article, single-point energy calculations have been performed by employing the higher-level MP2 calculations and larger 6-311+G(3df,2p) basis set to confirm the DFT results.

To analyze the geometrical changes caused by H_2O coordinating to the GC complexes, the stepwise binding energies of the following reactions

$$GC^{2+}\cdot(H_2O)_n + H_2O \rightarrow GC^{2+}\cdot(H_2O)_{n+1} \qquad (1)$$

are determined with eqn (2).

$$\Delta E_{adia} = E'_{g\text{-}c\text{-}w} - (E_{g\text{-}c\text{-}w} + E_w) + \Delta E_{cp} \qquad (2)$$

Here, n = 0–4 for the **1**-series while 0–5 for the **2**-series in reaction (1). In eqn (2), every item is defined as follows: ΔE_{adia} denotes the adiabatic binding energy; $E_{g\text{-}c\text{-}w}$ is the total energy of the glutamic acid–$Ca^{2+}\cdot(H_2O)_n$ complex corresponding to the relaxed geometries, while $E'_{g\text{-}c\text{-}w}$ denotes the total energy of the glutamic–$Ca^{2+}\cdot(H_2O)_{n+1}$ complex. E_w is the energy of the coordinated water molecules at the optimized geometries. All of these energies are corrected by ZPVE. Basis set superposition error (BSSE), presented as ΔE_{cp}, is computed through the counterpoise method[21] as implemented in Gaussian 03 code,[22] for all of the stable isomers of the GCW complexes, and is then used to correct the binding energies.

As a tentative study, the conformational and energetic behaviors of GCW in bulk water (the dielectric constant ε = 78.39) have been explored using the polarizable continuum model (PCM)[23–26] within the SCRF method at the same level employed in the gas phase.

In this article, ESP charge populations were determined at the B3LYP/6-311++G(2d,p) level of theory to investigate the polarization effects. Simultaneously, the VDW radius of Ca^{2+} required in the computation was cited from the *CRC*

Handbook of Chemistry and Physics.[27] On the other hand, the bonding molecular orbital contours and the harmonic vibrational frequencies have also been calculated at the same level of theory to explore the binding essence.

All of the calculations were performed using the Gaussian 03 suite of programs.[22]

3. Results and discussions

3.1. The first-shell coordination mode

3.1.1. Geometrical characterization. The optimized mono- to hexahydrated GC complexes with water in the first coordination shell of Ca^{2+} have been shown in Fig. 1, and the corresponding geometrical parameters are listed in Table 1. The binding enthalpies, entropies, and free energies are given in Table 2 for comparison. Notably, the presence of so many geometries for every hydration state seems to make the discussion very complicated. Simultaneously, the energy differences between them are very small. However, the important aim of this paper is to investigate the stepwise hydration effects on the geometrical and energetic behaviors of the amino acid–metal ion system. So only those geometries corresponding to the global minima on their respective potential energy surfaces (PES) by frequency analyses are selected in this paper. Obviously, the coordinated Ca–O bonds are elongated with the increase in water ligands, accompanied by the decrease of the (C–) O–Ca–O (–C) bond angles. Taking the hydrates of the **1**-series for example, the average Ca–O bond length of the non-hydrate is 2.33 Å, while this value increased gradually to 2.48 Å when the coordinated water molecules came to 5, indicating that the Ca–O bond strength has been weakened with the increase in ligands. Correspondingly, the (C–) O–Ca–O (–C) bond angle decreased from 57.0 to 52.3°. In fact, the contributions to the bond strength of the cation–ligand complexes can be roughly divided into several factors: (a) attractive electrostatic contributions, which include ion–dipole and ion-induced-dipole interactions and are expected to be the major contribution to the bond strength; (b) charge transfer from ligand to ion, which can be expected to be more significant for doubly, as compared to singly, charged ions and for more polarizable, strongly electron donating ligands; (c) electronic orbital effects such as ion core polarization and sd(σ) hybridization; (d) ion–ligand repulsion; and (e) ligand–ligand repulsion due to dipole–dipole and Pauli repulsion.[17] This last contribution can be expected to become more important with the increase in ligands in the first shell and will lead eventually to a transition to the first-and-second-shell binding mode. In fact, the geometrical changes of the GCW complexes can be explained completely from the viewpoints mentioned above. Firstly, the attractive electrostatic contribution is the main factor to trigger the Ca–O bonding, while the ion– and ligand–ligand repulsions can be expected to play a more dominant role as the CN increases and will lead eventually to the changes of the binding mode. Secondly, the charge transfer from the coordinated O to Ca^{2+} has also been investigated. In Table 3, the ESP charge populations, which can be used to investigate the polarized effects, are presented for the heavy atoms. Here, only those charges distributed on the calcium cation and the coordinated O atoms have been considered to explore the influence of the stepwise hydration on the GC complexes more effectively. For the **1**-series, it can be found intuitionally that the ESP distributions on the nucleophilic active sites are about 1.80 and the values are similar to the hydrates when the number of coordinated water molecules varies from 1 to 4, indicating that the hydration effects are similar on the polarization of the calcium cation in these hydrates. When the number of the coordination water molecules reaches 5, however, the ESP distribution on Ca^{2+} is much larger, corresponding to less charge transfer from ligand to cation. Thus, the electrostatic interaction between Ca^{2+} and O has been weakened. Thirdly, electronic orbital effects have also been extensively studied. For Ca^{2+}, it possesses empty 4s

Table 1 Selected geometrical parameters for the glutamic–$Ca^{2+}\cdot(H_2O)_n$ complexes[a]

Complex	R^{aver}(Ca–O)[b]	$R(N_1–H_{16})$	$R(O_9\cdots H_{16})$	$A(O_4–Ca_{20}–O_{10})$
1	2.33	1.09	1.52	57.0
1-w	2.36	1.08	1.54	56.4
1-2w	2.39	1.08	1.56	55.8
1-3w	2.42	1.07	1.58	54.9
1-4w	2.45	1.07	1.59	54.3
1-5w	2.48	1.07	1.60	52.3
1-3w · w	2.41	1.07	1.59	54.8
1-4w · w	2.44	1.07	1.60	53.9
1-2w · 2w	2.38	1.07	1.58	55.3
1-3w · 2w	2.41	1.07	1.60	54.6
Complex	R^{aver}(Ca–O)[b]	$R(N_1–H_{17})$	$R(O_8\cdots H_{17})$	$A(O_8–Ca_{20}–O_9)$
2	2.33	1.04	1.78	56.9
2-w	2.36	1.05	1.73	56.2
2-2w	2.39	1.06	1.68	55.6
2-3w	2.42	1.06	1.64	54.4
2-4w	2.45	1.07	1.60	53.8
2-5w	2.49	1.08	1.57	51.8
2-6w	2.54	1.09	1.53	50.6
2-3w · w	2.41	1.07	1.61	54.4
2-4w · w	2.45	1.08	1.57	53.4
2-5w · w	2.49	1.09	1.54	51.2
2-2w · 2w	2.37	1.06	1.63	55.1
2-3w · 2w	2.41	1.07	1.58	54.2
2-4w · 2w	2.45	1.09	1.53	53.2

[a] The bond lengths (R), bond angles (A) are in angstroms and degrees, respectively. Atom numbering used here is displayed in Fig. 1. [b] R^{aver}(Ca–O) is the average length of the Ca–O bonds.

Table 2 The calculated changes of enthalpy ΔH (in kcal mol^{-1}), entropy ΔS (in kcal mol^{-1} K^{-1}), Gibbs free energies ΔG (in kcal mol^{-1}), and hydrated energies (in kcal mol^{-1})

Reactions	ΔH	ΔS	ΔG	$\Delta E_{hydration}$
1 + w → **1-w**	−38.52	−0.023	−31.68	−39.45
1-w + w → **1-2w**	−32.92	−0.029	−24.19	−31.70
1-2w + w → **1-3w**	−28.17	−0.029	−19.42	−25.61
1-3w + w → **1-4w**	−21.68	−0.032	−12.24	−19.77
1-4w + w → **1-5w**	−19.19	−0.033	−9.49	−17.29
2 + w → **2-w**	−38.41	−0.024	−31.15	−35.35
2-w + w → **2-2w**	−33.47	−0.034	−23.28	−31.74
2-2w + w → **2-3w**	−28.15	−0.032	−18.64	−25.77
2-3w + w → **2-4w**	−22.03	−0.030	−13.05	−20.05
2-4w + w → **2-5w**	−18.31	−0.033	−8.54	−16.23
2-5w + w → **2-6w**	−11.04	−0.031	−1.76	−9.19

Table 3 ESP atomic charge distributions for glutamic–$Ca^{2+} \cdot H_2O$ complexes at the B3LYP/6-311++G(2d,p) level

	Atom numberings										
Hydrates	4	8	9	10	20	21	25	28	31	34	37
1-w	−0.68			−0.73	1.78	−1.09					
1-2w	−0.66			−0.71	1.77	−1.04	−1.05				
1-3w	−0.63			−0.66	1.77	−1.00	−1.03	−1.02			
1-4w	−0.66			−0.70	1.77	−0.93	−0.94	−1.01	−0.99		
1-5w	−0.69			−0.70	1.91	−0.98	−0.86	−1.01	−1.01	−0.99	
1-3w · w	−0.64			−0.75	1.76	−1.02	−1.05	−0.95	−0.83		
1-4w · w	−0.67			−0.65	1.75	−0.97	−0.90	−0.99	−1.00	−1.05	
1-2w · 2w	−0.70			−0.74	1.73	−1.02	−1.02	−0.77	−0.91		
1-3w · 2w	−0.63			−0.74	1.76	−1.04	−1.05	−0.96	−0.83	−0.88	
2-w		−0.94	−0.70		1.78	−1.10					
2-2w		−0.96	−0.70		1.80	−1.07	−1.09				
2-3w		−0.87	−0.69		1.79	−1.02	−1.01	−1.03			
2-4w		−0.91	−0.69		1.80	−0.97	−1.04	−1.00	−0.96		
2-5w		−0.89	−0.69		1.80	−0.89	−1.09	−0.95	−1.01	−0.80	
2-6w		−0.94	−0.75		1.87	−0.85	−0.97	−0.96	−0.95	−0.84	−0.90
2-3w · w		−0.99	−0.68		1.80	−1.06	−0.96	−1.07	−0.87		
2-4w · w		−0.91	−0.69		1.79	−0.96	−1.07	−1.00	−0.94	−0.91	
2-5w · w		−0.82	−0.68		1.84	−0.90	−1.15	−1.06	−0.92	−0.89	−0.85
2-2w · 2w		−0.91	−0.72		1.73	−1.03	−1.02	−0.78	−0.93		
2-3w · 2w		−0.96	−0.66		1.78	−1.05	−1.09	−0.96	−0.87	−0.88	
2-4w · 2w		−0.90	−0.69		1.76	−0.97	−0.91	−0.97	−0.89	−0.78	−0.80

and 4p orbitals and so can act as an acceptor to withdraw electron clouds from the coordinated oxygen atoms. Obviously, in addition to the electrostatic interaction between the Ca^{2+} cation and the negative charge over the coordination centers, the orbital coupling is also an important contribution to the bonding between Ca^{2+} and the coordination ligands. Here, the several different orbital coupling modes for the Ca–O bonding have been shown diagrammatically in Fig. 2, and the orbital energy levels associated directly with Ca^{2+} bonding properties have also been compared in Fig. 3. Obviously, Ca^{2+} uses its hybrid (4s,4p) orbitals to interact with the ligand orbitals, and the composition of these hybrid orbitals may vary subject to the coupling modes between Ca^{2+} and the ligands, so the careful inspection into the bonding orbitals of these complexes could give a basis for analyzing the binding between Ca^{2+} and the ligands. For the isomer **1**, when no water molecule is coordinated, its HOMO and HOMO-1 describe the bonding character of the free –COOH group, and no coupling interaction associated with the Ca^{2+} ion exists. However, the HOMO-2 and HOMO-3 orbitals do describe the σ_2-type $\sigma Ca–O_4$ and $\sigma Ca–O_{10}$ bonding and π_1-type $\pi Ca–O_4$ and $\pi Ca–O_{10}$ bonding nature. After one water molecule is coordinated to the GC complex, the electronic distributions of the coordinated orbitals have changed a lot. The HOMO of **1-w** exhibits almost the same shape compared with that in **1**, but the overlapping degree of the coordinated Ca–O bonds in **1-w** has increased. This phenomenon has been verified further in the HOMO-1: although exhibiting the similar –COOH bonding character to **1**, the greater Ca–O bond overlapping indicates that the hydration makes the distribution of the electron clouds of the whole coordination system move to the Ca–O coordination center because of the increased electrostatic interaction. Similar to the geometry **1**, the orbitals of HOMO-2 and HOMO-3 have also exhibited the σ_2- and π_1-type coordination bonding but more orbital couplings have been moved to the Ca–O coordination site correspondingly. The similar phenomena mentioned above have appeared in **1-2w**. Simultaneously, another notable phenomenon has also been found: the HOMO-1 of **1-2w** exhibits a similar orbital distribution, which describes the Ca–O coordination character, to HOMO-2 in **1-w**, indicating that the orbital energy levels associated with Ca^{2+} bonding properties move up to the more frontier zone with the increase in coordinated water molecules. Obviously, the higher energy of Ca^{2+}-coupling has also resulted in the decrease of the Ca–O bonding strength.

All in all, the integration of the ion– and ligand–ligand interactions, charge transfer and electronic orbital effects has determined the decreased strength of the Ca–O bonding.

As another important indicator to describe the changes caused by the hydration, the intramolecular H-bond, $N_1–H_{16}\cdots O_9$, which is the most characteristic vibrating mode in the **1**-series, has also been extensively studied. As shown in Table 1, the length of $N_1–H_{16}$ decreases monotonely (from 1.09 Å in **1** to 1.07 Å in **1-5w**) with the increase in coordinated water molecules, indicating the larger bonding strength between these two atoms. This phenomenon can be confirmed by the blue-shift of about 300 cm^{-1} (from 2444 cm^{-1} in **1** to 2732 cm^{-1} in **1-5w**) for the stretching vibration between N_1 and H_{16} (see Fig. 4). Correspondingly, the strength of $O_9–H_{16}$ has been weakened. Then, what has made these changes? As discussed hereinbefore, the increase in water molecules has weakened the Ca–O bonding strength, thus increasing the basicity of the carboxylic O_{10}. Correspondingly, H_{19} is attracted more strongly by O_{10} and away from N_1, resulting in the increased basicity of N_1. Thus, this nitrogen atom possesses of larger capability to bond H_{16}, which in turn decreases the bond length of $O_9\cdots H_{16}$.

When investigating the hydrations of the **2**-series, which denote another GC coupling mode, we have found that most

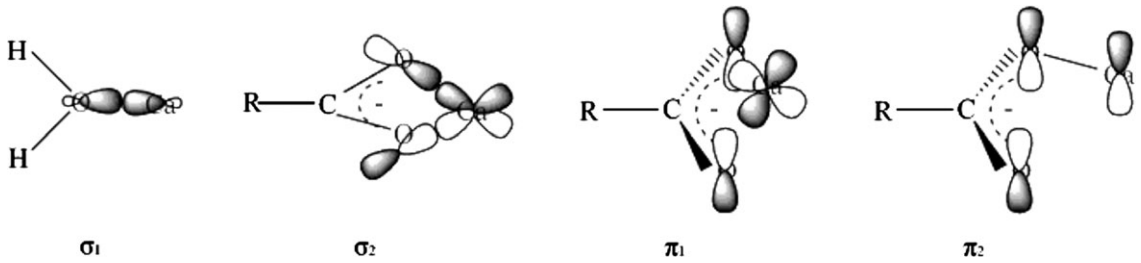

Fig. 2 The modelling orbital coupling contours for the interaction between Ca^{2+} and the active groups in glutamic acid and water ligands.

of the geometrical characters are similar to those in the **1**-series except for several interesting phenomena. One is the existence of the hexahydrate of the **2**-series (**2-6w**), in which the glutamic acid ligand remains to be bidentate coupling to Ca^{2+}, while the corresponding hexahydrate of the **1**-series cannot be found after all kinds of attempts. The careful ESP investigation has implied a valuable clue to explain this discrepancy. As can be found in Table 3, the electrostatic distributions on Ca^{2+} are similar to the **1**- and **2**-series for $n = 0$–4, while in **1-5w** the charge distribution on Ca^{2+} is markedly larger than that in **2-5w**. Thus, it can be speculated that the coordinated oxygen atoms contribute less electrons to the Ca^{2+} ion in **1-5w**, resulting in the weaker Ca–O bonding and the smaller overlapping of the electron clouds among the coordinated atoms of **1-5w** than **2-5w**. When more ligands participate in the coordination, the Ca–O (–C) bond of **1-6w** breaks easily, but **2-6w** can retain the glutamic acid ligand to couple to Ca^{2+} bidentately. Another notable phenomenon is that the characteristic frequency, the N_1–$H_{17}\cdots O_8$ stretching one, has taken on the red-shift changes with the increase in coordinated water molecules (Fig. 4). Although contrary to the blue-shift phenomenon of the characteristic vibrations in the **1**-series, the frequency changes of the **2**-series can also be understood from the aspects of the electrostatic interaction, ion– and

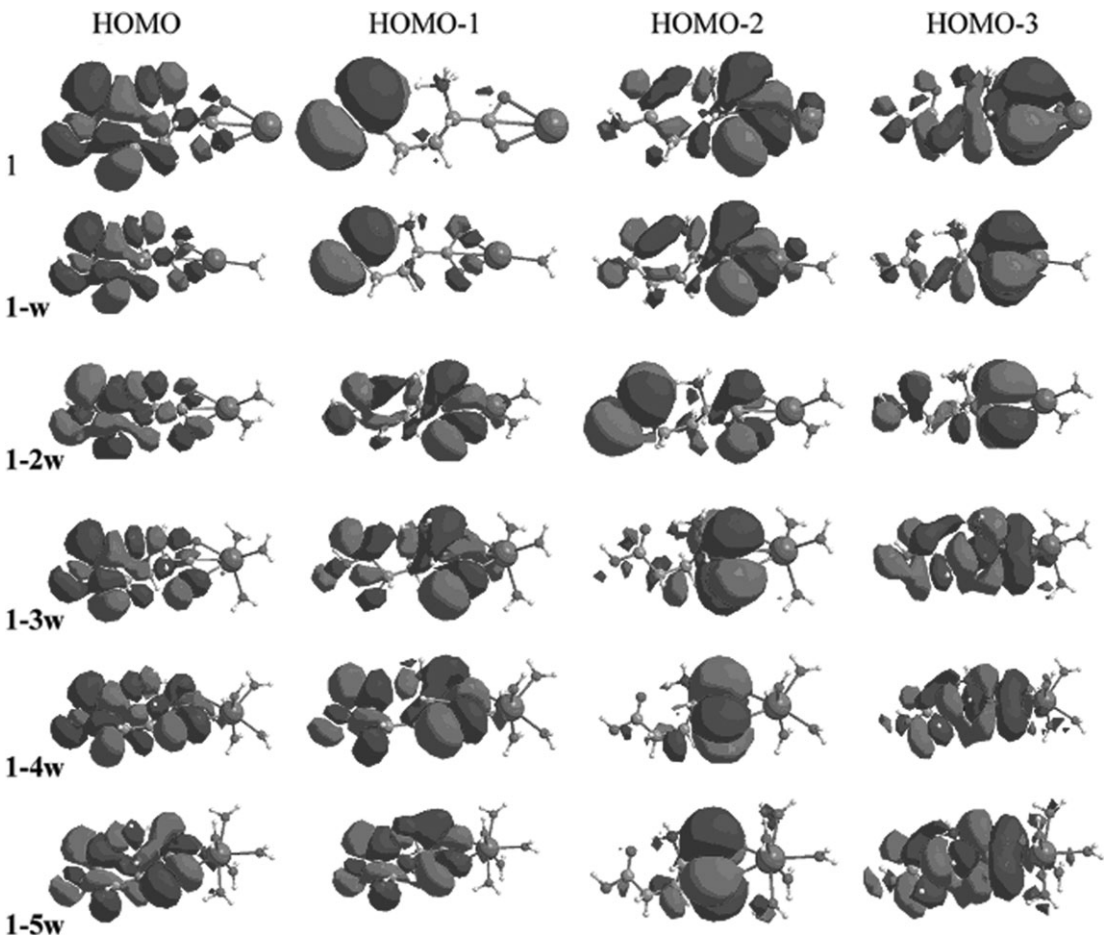

Fig. 3 Diagrams of high energy level orbitals for the glutamic–$Ca^{2+}\cdot(H_2O)_n$ ($n = 0$–5) complex of the **1**-series. Isocontour value 0.01 is used. The order is HOMO, HOMO-1, HOMO-2 and HOMO-3 from left to right.

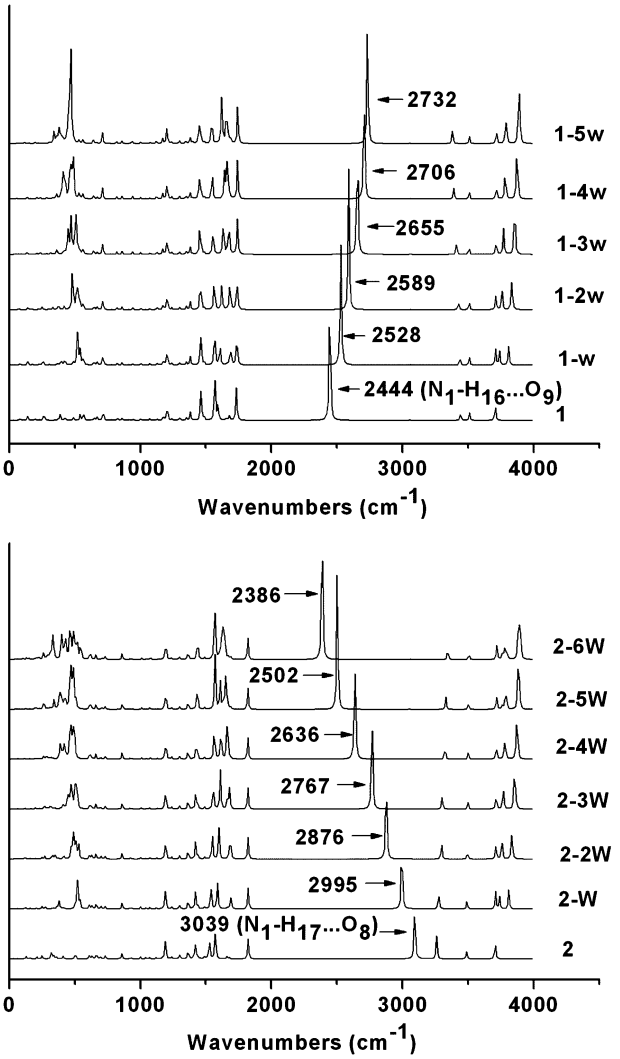

Fig. 4 IR spectra of the first-shell hydrates corresponding to the **1**- and **2**-series, respectively, obtained at the B3LYP/6-311++G(2d,p) level. The wavenumbers pointed out specially are the characteristic vibrations.

ligand–ligand repulsions, charge transfer from ligand to ion and the electronic orbital effects. With the increase in coordinated ligands, the ion– and ligand–ligand repulsions have made the calcium and oxygen atoms detach from each other as far apart as possible. Simultaneously, this has also resulted in less charge transfer from the oxygen atoms to the calcium ion verified by the ESP atomic charge distributions on Ca^{2+} (increasing from 1.78 to 1.87 corresponding to the coordinated water increasing from 1 to 6 in the first shell). On the other hand, the bonding analysis has shown that the orbital overlap between Ca^{2+} and the coordinated oxygen atoms moves to the higher energy level gradually with the increase in ligands, in good agreement with the weakened Ca–O bonding (see Fig. S2†). As a whole, these aspects have made more electrons distribute on O_8, thus increasing its basicity. Then H_{17} has received stronger attractions coming from this oxygen atom and the corresponding N_1–H_{17} bond has certainly been weakened. Noticeably, the characteristic N–H stretching vibrations occur at the high frequencies and correspond to the great intensities, so the experimenters can entirely use these investigatory results to designate the correlating active groups.

3.1.2. Energy analyses. Table 2 summarizes the calculated hydration energies (ΔE), ΔH, ΔS, and ΔG (with the ZPVE and BSSE corrections) in the hydration process corresponding to the following reactions:

$$GC^{2+}\cdot(H_2O)_n + H_2O \rightarrow GC^{2+}\cdot(H_2O)_{n+1} \qquad (1)$$

Here, n = 0–4 for the **1**-series, while n = 0–5 for the **2**-series.

Inspecting the five reactions of the **1**-series, similar thermodynamic characters can be found. Taking the hydration reaction **1** + w → **1-w** for example: this reaction is enthalpy-favored, because $\Delta H = -38.52$ kcal mol^{-1}; on the other hand, the binding of a water molecule to the first coordination shell of Ca^{2+} results in an unfavorable entropic term ($T\Delta S = -6.83$ kcal mol^{-1}). However, the whole reaction is enthalpy-driven ($\Delta G = -31.68$ kcal mol^{-1}) because of the relatively small value of ΔS.

On the other hand, as we can see from Table 2, the values of ΔH for the **1**-series range from −38.52 to −19.19 kcal mol^{-1} with the water molecules increasing from 1 to 5, indicating that the stepwise hydration reactions become less favorable. Additionally, the gradual increase of the negative values of ΔS has shown the decrease of the degree of chaos, which also disfavors the progress of the reactions to the positive direction. Thus, the changes of ΔG values (from −31.68 to −9.49 kcal mol^{-1}) have also shown the more unfavorable character of the stepwise hydration processes with the increase in ligands. When the coordinated water molecules reach a certain number, it can be speculated that the further hydration remaining the bidentate coordination mode of the glutamic acid to Ca^{2+} will be enthalpy-unfavorable. In our study, this number should be 6 because the corresponding hexahydrate remaining the glutamic acid coupling to Ca^{2+} bidentately cannot be found after many endeavours. The hexahydrate can only be obtained by freeing a bound carboxylic oxygen atom to accommodate the sixth water molecule in the first coordination shell. As for the hydration energies, the gradually decreased values have suggested that the further hydration will stabilize the ion–ligand system.

For the **2**-series, the hydration characters are similar to the **1**-series except for the irregular changes of ΔS. However, the so small values of the degree of chaos have little influence on ΔG, verifying again that the reactions are enthalpy-driven. Notably, the free energy is very small ($\Delta G = -1.76$ kcal mol^{-1}) when the coordinated H_2O increases from 5 to 6, suggesting that further hydration may result in positive values of ΔG, then the heptahydrate remaining the glutamic acid coupling to Ca^{2+} bidentately would not be found. Surely, the endeavours of adding the seventh water molecule to the first shell have resulted in the break of a Ca–O (–C) bond in our study.

3.2. The first-and-second-shell coordination mode

3.2.1. Geometrical characterization. To investigate the hydration effects more elaborately, we have designed two kinds of peripheral hydration modes. One is the (n, 1) mode (n = 3,

Table 4 The selected geometrical parameters of (3,0), (3,1), and (3,2) modes corresponding to the **1**- and **2**-series, respectively[a]

Complex	R(Ca–O)	R(N_1–H_{16})	R($O_9\cdots H_{16}$)	A(O–Ca–O)
1-3w	2.418	1.07	1.58	54.9
1-3w · w	2.412	1.07	1.59	54.8
1-3w · 2w	2.410	1.07	1.60	54.6
Complex	R(Ca–O)	R(N_1–H_{17})	R($O_8\cdots H_{17}$)	A(O–Ca–O)
2-3w	2.416	1.06	1.64	54.4
2-3w · w	2.410	1.07	1.61	54.4
2-3w · 2w	2.406	1.07	1.58	54.2

[a] The bond lengths (R), bond angles (A) are in angstroms and degrees, respectively. Atom numbering used here is displayed in Fig. 1.

4 for the **1**-series and 3, 4, 5 for the **2**-series), and another is the (n, 2) mode (n = 2, 3 for the **1**-series and 2, 3, 4 for the **2**-series) because the familiar CN of the calcium cation *in vivo* varies from 6–9, as reported by the previous papers.[12] In all of the optimized results, those geometries with the second-shell water molecules coordinating to the first-shell ones using as many H-bonds as possible are the most stable forms. Obviously, the H-bonds have played an important role in stabilizing the hydrates. To explore the peripheral hydration effects on the GC complexes in detail, we have compared the geometrical changes among the hydrates with the same hydration number in the first shell but a different number of peripheral waters, such as **2-3w**, **2-3w · w**, and **2-3w · 2w**. The selected geometrical parameters including the average Ca–O bond lengths, characteristic H-bond lengths, and (C–) O–Ca–O (–C) bond angles are listed in Table 4 (more detailed comparisons are shown in Table S1 of the ESI†), from which, several clear trends can be concluded. The average Ca–O bond lengths, compared among the (3, 0), (3, 1) and (3, 2) modes of the **2**-series, are shortened with the increase in peripheral waters. In fact, these changes come from the decrease of the Ca–O (–H) bond lengths, that is, the peripheral hydration has made the first-shell water molecules bind more strongly to the calcium ion. This has made the Ca–O (–C) bond lengths take on the increasing trend. For example, the average Ca–O bond lengths in **2-3w**, **2-3w · w**, and **2-3w · 2w** are 2.416, 2.410, and 2.406 Å, respectively, and the corresponding Ca–O (–H) ones are 2.413, 2.40, and 2.390 Å, while the average lengths of Ca–O (–C) bonds are 2.420, 2.425 and 2.430 Å. Resulting from these changes in the bond lengths, the (C–) O–Ca–O (–C) bond angles become smaller with the increase in peripheral water molecules. As for the characteristic N_1–H_{17} bonds, the corresponding bond lengths are almost the same although the IR analysis has shown the red-shift phenomenon for the stretching vibration, with the frequency changing from 2767 to 2689 then to 2594 cm^{-1}. In fact, the peripheral hydration has very small effect on the coordination characters of the GC complex verified by the bond analysis (Fig. S3 of the ESI†). Here, we have also found another interesting phenomenon: the magnitude of the bond length shortenings becomes smaller with the quantitative addition of peripheral water molecules, indicating that the calcium cation and the ligands become less sensitive to the outer environment.

3.2.2. Energy analyses. The main interaction of the ion–ligand complex, as we have known, is an electrostatic one, which has driven the electronegative atoms to bind to the metal ions. However, this binding capability is not limitless because of the increased ion– and ligand–ligand repulsions. Then, what is the optimal CN of Ca^{2+} for the GC complexes and how do the different factors influence the coordination modes? To answer these questions, we have designed the following project. When the calcium cation is surrounded by three water molecules in the first shell, that means, the CN of Ca^{2+} is five, there would be two ways for the fourth water molecule to bind to glutamic acid–$Ca^{2+}\cdot(H_2O)_3$: one is to bind in the first shell sequentially, and another is to bind in the second shell. Then, we can get some useful information about the preferred coordination geometry and the correlating energetic changes by comparing the relative energies among the (n, 0), (n − 1, 1), and (n − 2, 2) (n = 4, 5 for the **1**-series and 4, 5, 6 for the **2**-series) forms. All of the corresponding energies calculated at the B3LYP/6-311++G(2d,p) level are listed in Table 5. Taking the **2**-series for example, upon the most stable trihydrate, the fourth water molecule prefers to bind to **2-3w** in the first coordination shell rather than in the second one, with the energy of **2-4w** (CN = 6) being 1.8 kcal mol^{-1} lower than that of **2-3w · w** (CN = 5). The corresponding (2, 2) mode (CN = 4), which is unstable, is 10.3 kcal mol^{-1} higher in energy than that of **2-4w**. This energetic discrepancy has indicated that the hexacoordinated form to Ca^{2+} is more stable than the pentacoordinated one in the first shell. Further, when the fifth water is coordinated to the complex, the ability of this water molecule to bind in the second shell (CN = 6) is larger than in the first one (CN = 7) with the energetic discrepancy being 1.1 kcal mol^{-1}. Again, the 3.8 kcal mol^{-1} higher energy of **2-3w · 2w** (CN = 5) than that of **2-4w · w** verifies that the pentacoordinated form for the calcium cation in the first shell is unstable. As to the hexahydrates, the complex with CN = 6 is still the optimal with the energy being only 0.9 kcal mol^{-1} lower than **2-5w · w** (CN = 7). Simultaneously, the complex corresponding to CN = 8 is very unstable (7.4 kcal mol^{-1} higher in energy than that of **2-4w · 2w**). Thus, the analyses above have shown that the optimal CN of Ca^{2+} in the gas phase is 6. However, the comparison of the relative energies among **1-5w**, **1-4w · w** and **1-3w · 2w** has suggested that 7 may also be another optimal CN of Ca^{2+}. In fact, the previous papers have confirmed these conclusions.[6,12–14] For example, Dudev *et al.* have suggested that the average CN of Ca^{2+} is 6 in proteins.[6] However, for the most frequent Ca^{2+}-binding motif in soluble proteins, which is EF-hand, the average CN is 7.[13] Obviously, the relative energies (in Table 5) of different complexes lie within a small range and may be quite sensitive to the methodology used. To further verify the reliability of the conclusions in this paper, single-point energy calculations on the representative (5,0) (4,1) and (3,2) modes of the **1**- and **2**-series have been performed by employing the more accurate 6-311+G(3df,2p) basis set and the higher-level MP2 method. For the **1**-series, the calculated results at the different levels are well consistent with each other. For the **2**-series, although the calculated results at the MP2/6-311++G(2d,p) and MP2/6-311+G(3df,2p) levels listed in Table S2† give a different order in relative energies to those of the B3LYP/6-311++G(2d,p)

Table 5 Energy differences ΔE (kcal mol^{-1}) among the (n, 0), ($n-1$, 1), and ($n-2$, 2) (n = 4 and 5 for the **1**-series while 4 ~ 6 for the **2**-series) forms obtained at the B3LYP/6-311++G(2d,p) level plus ZPVE corrections

Complex	ΔE	Complex	ΔE
1-4w	0.0	**1-5w**	0.0
1-3w · w	+1.8	**1-4w · w**	+0.2
1-2w · 2w	+10.3	**1-3w · 2w**	+3.4

Complex	ΔE	Complex	ΔE	Complex	ΔE
2-4w	0.0	**2-5w**	+1.1	**2-6w**	+7.4
2-3w · w	+1.8	**2-4w · w**	0.0	**2-5w · w**	+0.9
2-2w · 2w	+10.3	**2-3w · 2w**	+3.8	**2-4w · 2w**	0.0

level of theory, they have also indicated one of the optimal CN of Ca^{2+}, which is 7, in accordance with the conclusion drawn in this paper. So, the consistency between DFT and higher-level methods can be confirmed. In addition, the reliability of the DFT/B3LYP method has also been discussed in dealing with the Ca^{2+}-associated system.[28] In this paper, the authors found that this method can provide a good compromise between accuracy and computational cost in the calculation of the geometries and binding energies.

In order to further elucidate the geometrical and energetic behaviors of the GC complexes in the bulk solution, the PCM within the SCRF method at the same level used in the gas phase has been employed. The selected solvent is water with the dielectric constant ε = 78.39. Here, only representative **2-5w**, **2-4w · w** and **2-3w · 2w** are discussed. The SCRF calculations reveal that **2-5w** (CN = 7) is the most stable form, with the energy being 1.9 and 5.4 kcal mol^{-1} lower than those of **2-4w · w** (CN = 6) and **2-3w · 2w** (CN = 5), respectively. Thus, the optimal CN may be 7 in the bulk solution. The same phenomena have appeared in the complexes of the **1**-series.

As discussed hereinbefore, the stability of the GCW complexes can be attributed to the electrostatic interaction and the ion– and ligand–ligand repulsions. The former factor, which is dominant when the number of coordinated water molecules is small, upholds the first-shell coordination mode, while the latter one approves of the second shell mode. So, when the number of coordinated ligands in the first-shell acquires the saturated state, the additional water molecules would bind spontaneously to the second shell. Obviously, three important conclusions can be drawn from the above analyses: (i) the preferred CN of the GCW system is 6 or 7, agreeing with the data reported in the previous papers.[6,12–14] However, this value will become 7 calculated at the higher-level MP2 level. (ii) The energetic discrepancy between the hydrates with CN = 6 and 7 become smaller with the quantitative increase in coordinated waters (in Table 5), and the heptacoordinated complex can become the most stable form in the bulk solvent. This point has been verified by the SCRF calculations. Additionally, so small an energetic discrepancy has shown that the hexa- and heptacoordinated forms are almost isoenergetic with the number of the ligands increasing, reflecting the complicated Ca^{2+}-coupling forms in bulk solvent. (iii) The CN of Ca^{2+} in the first coordination shell cannot increase limitlessly with the addition of the water molecules. Obviously, this is mainly owing to the equilibrium of the electrostatic interaction and ion– and ligand–ligand repulsions, as mentioned above.

3.3. The implications to the Ca^{2+}-channel

In our studies, the water molecule in glutamic acid–$Ca^{2+} \cdot (H_2O)_n$ complex can be analogized as another amino acid molecule or a simple peptide, just like the real biological system. Furthermore, glutamic acid–$Ca^{2+} \cdot (H_2O)_n$ can become a larger steric peptide or protein if other amino acids substitute for the water molecules to attach the Ca^{2+} end. In the previous studies, Sugita *et al.* have reported that Ca^{2+} is coordinated by 7 oxygen atoms with different geometries in both of the two high-affinity sites in Ca^{2+}-ATPase.[14] Costa and Carloni have pointed out, however, that the CN of Ca^{2+} for these two sites are 8.4 ± 0.6 and 8.1 ± 0.3 through molecular modelling.[5] In this paper, the energetic analyses have shown that both 6 and 7 are the possible CN in the gas phase. Furthermore, the energetic discrepancy of hexa- and heptacoordinated complexes is smaller with the increase in coordination ligands, and the heptacoordinated form can become the favorite one in the bulk solvent verified by the SCRF calculations. Obviously, the findings of Sugita *et al.* can be reproduced by the present studies, suggesting that GC is a good model to mimic the coordinated characters of Ca^{2+}–amino acid complexes in Ca^{2+}-ATPase. As to the octacoordinated form, the much higher energy than that of the hexa- and heptacoordinated complexes has suggested that its possibility of existing in the Ca-binding protein is very rare.

In the process of stepwise addition of water molecules to the GC complexes, the lengthened Ca–O (–C) bonds would break, thus the coordinated water molecules will replace the amino acid partly or entirely. Simultaneously, the results have shown the changes of the coupling mode of the amino acid between two fundamentally different biological binding mechanisms (from the inner-sphere mode to the outer-sphere one). For example, **1-5w** and **1-6w** shown in Fig. 5 represent the two kinds of inner-sphere binding mode for the amino acid, while **1-7w** represents the outer-sphere form, in which the glutamic acid exists in the second shell of Ca^{2+} and is stabilized *via* the strong hydrogen bonds to the first-shell coupling water molecules. Considering the fact that, in Ca^{2+}-ATPase, the water molecules will replace the coupled amino acid residues partly

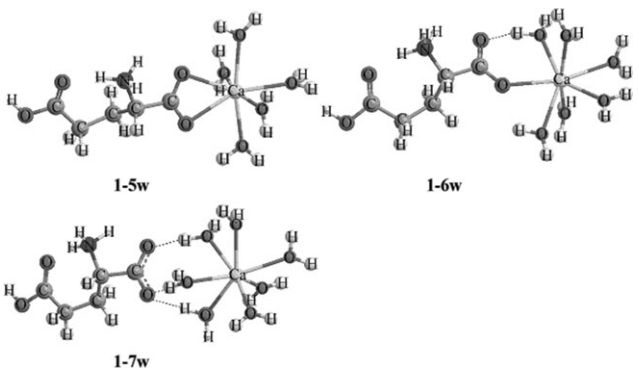

Fig. 5 The inner-sphere (**1-5w** and **1-6w**) and the outer-sphere binding mode (**1-7w**) of the glutamic acid ligand to Ca^{2+}.

Table 6 The average Ca–O bond lengths for the different systems[a]

System	**1-5w**	**2-5w**	Ca-7w[b]	Ca(I)–Ca_2E_1[c]	Ca(II)–Ca_2E_1[c]	Ca(I)-X-ray[d]	Ca(II)-X-ray[d]
R^{aver}(Ca–O)	2.48 (2.47[e])	2.49 (2.46[e])	2.49 (2.45[e])	2.7 ± 0.1	2.6 ± 0.2	2.36	2.43

[a] The bond lengths (R) are in angstroms. [b] This datum derives from our calculations. [c] The data derive from the molecular modelling results in ref. 5. [d] The data are extracted from the X-ray structures in ref. 1. [e] The data in the parenthesis are the results of the SCRF calculations.

or entirely when Ca^{2+} releases from the high-affinity sites to the lumen side, the ligand exchange taking place in our study can be analogized to this release process. The corresponding thermodynamics parameters of the hydration reactions **1-5w** + w → **1-6w** and **1-6w** + w → **1-7w** have shown that these two hydration processes accompanied by the breaks of the Ca–O (–C) bonds are free energy-supported with $\Delta G = -5.2$ and -1.9 kcal mol^{-1}, respectively. On the other hand, such small energies have also indicated that the release and binding processes of Ca^{2+} *in vivo* are subtle and the binding/release equilibrium can be reached more easily.

On the other hand, the differences between the model system considered here and the Ca^{2+}-channel should also be mentioned. In Table 6, we have compared the average Ca–O bond lengths of $Ca^{2+} \cdot (H_2O)_7$, glutamic–$Ca^{2+} \cdot (H_2O)_5$ calculated in this paper, and the two high-affinity sites of Ca^{2+} in the Ca^{2+}-ATPase extracted from the X-ray structure (PDB code: 1SU4)[1] and those calculated by molecular modelling.[5] Obviously, the average Ca–O bond lengths derived from the theoretical calculation are larger than those from the experiment. However, our calculated results, especially those from the SCRF calculations, are more approximate to that of site II in the X-ray structure of Ca^{2+}-ATPase. Notably, the interaction of Ca^{2+}–amino acid in Ca^{2+}-channel is a very complex process, so the substituting of the amino acid ligands with the water molecules simply can only mimic the real biological system to a certain extent. However, the present work can surely supply some useful information to recognize the hydration effect on the metal ion–amino acid system, and elucidate some biological phenomena correlating with the Ca^{2+}-channel *in vivo*.

4. Conclusions

In the present paper, the hydration processes to the GC complexes have been investigated systematically by employing the B3LYP density functional theory method with the 6-31+G(d,p) and 6-311++G(2d,p) basis sets. The principal conclusions from this study are as follows.

1. The stepwise hydration has caused a series of geometrical changes about the GC complexes. In the first-shell and first-and-second-shell coordination modes, these changes are different. Influenced by the ion–ligand electrostatic interaction, charge transfer from ligand to ion, electronic orbital effects, ion– and ligand–ligand repulsions, the increase of the water molecules in the first shell has weakened the Ca–O bond strength, which also results in the decrease of the (C–)O–Ca–O(–C) bond angles. Notably, in the first-and-second-shell coordination mode, the peripheral hydration has caused the calcium cation to move closer to the first-shell water molecules, but increased the distance between Ca^{2+} and the carboxylic oxygen atoms.

2. The interactive energies calculated in the gas phase have indicated that the optimal CN of Ca^{2+} is 6 or 7, while in the bulk water, this value is 7, indicating the complicated existing state of the Ca^{2+}-coupling system. Furthermore, the calculations employing the more accurate basis set and higher-level MP2 method have also confirmed this conclusion. Simultaneously, the studies about the thermodynamics parameters have shown that the stepwise hydration is enthalpy-driven because of the very small value of ΔS.

3. When the number of coordinated water molecules reaches 6 or 7, the lengthened Ca–O (–C) bonds would break sequentially, thus the coordinated water will replace the amino acid partly or entirely. This replacement results in the transformation between two fundamentally different biological binding mechanisms of the amino acid–metal ion system (the inner- and outer-sphere modes), just like the real process of Ca^{2+} release from the high-affinity sites into the lumen side in the Ca^{2+}-channel. The small values of ΔG (-5.2 and -1.9 kcal mol^{-1}) in the hydration reactions have suggested that the release and binding processes of the calcium cation *in vivo* can reach the equilibrium state relatively easily.

4. The model of the GCW complexes can reveal some disciplines of the Ca^{2+}-channel partly, but not completely, because the active transport of Ca^{2+} across biological membranes is a very complex process *in vivo*. Nevertheless, we hope the calculated data will be useful for experimental and theoretical studies. Additionally, further investigation is in progress.

Acknowledgements

This work is supported by NSFC (20573063, 20273040), NIH (Grant No. GM62790), NCET and the NSF of Shandong Province (Z2003B01), SRFD, SCF for ROCS-SEM, and the project of ChinaGrid. Support from the Virtual Laboratory for Computational Chemistry of CNIC and the Supercomputing Center of CNIC-CAS is also acknowledged. Part of the calculations was performed on the Center for Biological Modeling and the Michigan Center for Biological Information Linux clusters at Michigan State University, and the High-performance Computational Center in Shandong University. The author (YB) also thanks Prof. Yi Hu for his help in calculations.

References

1 C. Toyoshima, M. Nakasako, H. Nomura and H. Ogawa, *Nature*, 2000, **405**, 647.
2 (*a*) A. G. Lee and J. M. East, *Biochem. J.*, 2001, **356**, 665; (*b*) A. G. Lee, *Curr. Opin. Struct. Biol.*, 2002, **12**, 547.

3 C. Xu, W. J. Rice, W. He and D. L. Stokes, *J. Mol. Biol.*, 2002, **315**, 201.
4 T. L. Sørensen, J. V. Møller and P. Nissen, *Science*, 2004, **304**, 1672.
5 V. Costa and P. Carloni, *Proteins: Struct., Funct., Genet.*, 2003, **50**, 104.
6 (*a*) T. Dudev and C. Lim, *J. Phys. Chem. B*, 2004, **108**, 4546; (*b*) C. S. Babu, T. Dudev, R. Casareno, J. A. Cowan and C. Lim, *J. Am. Chem. Soc.*, 2003, **125**, 9318; (*c*) T. Dudev, Y. Lin, M. Dudev and C. Lim, *J. Am. Chem. Soc.*, 2003, **125**, 3168; (*d*) T. Dudev and C. Lim, *Chem. Rev.*, 2003, **103**, 773; (*e*) T. Dudev and C. Lim, *J. Am. Chem. Soc.*, 2006, **128**, 1553.
7 F. Xiang, Y. Bu, H. Ai and P. Li, *J. Phys. Chem. B*, 2004, **108**, 17628.
8 R. A. Jockusch, A. S. Lemoff and E. R. Williams, *J. Phys. Chem. A*, 2001, **105**, 10929.
9 H. Einspahr and C. E. Bugg, *Acta Crystallogr., Sect. B: Struct. Crystallogr. Cryst. Chem.*, 1981, **B37**, 1044.
10 C. J. Carrell, H. L. Carrell, J. Erlebacher and J. P. Glusker, *J. Am. Chem. Soc.*, 1988, **110**, 8651.
11 E. E. Abola, J. L. Sussman, J. Prilusky and N. O. Manning, *Methods Enzymol.*, 1997, **277**, 556.
12 W. Yang, L. M. Jones, L. Isley, Y. Ye, H.-W. Lee, A. Wilkins, Z.-r. Liu, H. W. Hellinga, R. Malchow, M. Ghazi and J. J. Yang, *J. Am. Chem. Soc.*, 2003, **125**, 6165.
13 E. Pidcock and G. R. Moore, *JBIC, J. Biol. Inorg. Chem.*, 2001, **6**, 479.
14 Y. Sugita, N. Miyashita, M. Ikeguchi, A. Kidera and C. Toyoshima, *J. Am. Chem. Soc.*, 2005, **127**, 6150.
15 M. I. Bernal-Uruchurtu and I. Ortega-Blake, *J. Chem. Phys.*, 1995, **103**, 1588.
16 (*a*) A. D. Becke, *J. Chem. Phys.*, 1993, **98**, 5648; (*b*) C. Lee, W. Yang and R. G. Parr, *Phys. Rev. B: Condens. Matter Mater. Phys.*, 1988, **37**, 785; (*c*) P. J. Stevens, F. J. Devlin, C. F. Chablowski and M. J. Frisch, *J. Phys. Chem.*, 1994, **98**, 11623.
17 M. Peschke, A. T. Blades and P. Kebarle, *J. Am. Chem. Soc.*, 2000, **122**, 10440.
18 G. Tiraboschi, B. Roques and N. Gresh, *J. Comput. Chem.*, 1999, **20**, 1379.
19 A. C. Tsipis, C. A. Tsipis and V. Valla, *J. Mol. Struct. (THEOCHEM)*, 2003, **630**, 81.
20 H. Ai and Y. Bu, *J. Phys. Chem. B*, 2004, **108**, 1241.
21 M. J. Frisch, J. E. Del Bene, J. S. Binkley and H. F. Schaefer III, *J. Chem. Phys.*, 1986, **84**, 2279.
22 M. J. Frisch, G. W. Trucks, H. B. Schlegel, G. E. Scuseria, M. A. Robb, J. R. Cheeseman, J. A. Montgomery, Jr, T. Vreven, K. N. Kudin, J. C. Burant, J. M. Millam, S. S. Iyengar, J. Tomasi, V. Barone, B. Mennucci, M. Cossi, G. Scalmani, N. Rega, G. A. Petersson, H. Nakatsuji, M. Hada, M. Ehara, K. Toyota, R. Fukuda, J. Hasegawa, M. Ishida, T. Nakajima, Y. Honda, O. Kitao, H. Nakai, M. Klene, X. Li, J. E. Knox, H. P. Hratchian, J. B. Cross, C. Adamo, J. Jaramillo, R. Gomperts, R. E. Stratmann, O. Yazyev, A. J. Austin, R. Cammi, C. Pomelli, J. W. Ochterski, P. Y. Ayala, K. Morokuma, G. A. Voth, P. Salvador, J. J. Dannenberg, V. G. Zakrzewski, S. Dapprich, A. D. Daniels, M. C. Strain, O. Farkas, D. K. Malick, A. D. Rabuck, K. Raghavachari, J. B. Foresman, J. V. Ortiz, Q. Cui, A. G. Baboul, S. Clifford, J. Cioslowski, B. B. Stefanov, G. Liu, A. Liashenko, P. Piskorz, I. Komaromi, R. L. Martin, D. J. Fox, T. Keith, M. A. Al-Laham, C. Y. Peng, A. Nanayakkara, M. Challacombe, P. M. W. Gill, B. Johnson, W. Chen, M. W. Wong, C. Gonzalez and J. A. Pople, *GAUSSIAN 03 (Revision B.05)*; Gaussian, Inc., Pittsburgh, PA, 2003.
23 E. Cancès, B. Mennucci and J. Tomasi, *J. Chem. Phys.*, 1997, **107**, 3032.
24 M. Cossi, V. Barone, B. Mennucci and J. Tomasi, *Chem. Phys. Lett.*, 1998, **286**, 253.
25 B. Mennucci and J. Tomasi, *J. Chem. Phys.*, 1997, **106**, 5151.
26 M. Cossi, G. Scalmani, N. Rega and V. Barone, *J. Chem. Phys.*, 2002, **117**, 43.
27 *CRC Handbook of Chemistry and Physics*, ed. D. R. Lide, CRC Press, Cleveland, 82nd edn, 2001–2002.
28 I. Corral, O. Mó, M. Yáñez, A. P. Scott and L. Radom, *J. Phys. Chem. A*, 2003, **107**, 10456.

